Journal of Environmental Management 390 (2025) 126344

Contents lists available at ScienceDirect

Journal of Environmental Management

journal homepage: www.elsevier.com/locate/jenvman

Research article

DNDC modelling of greenhouse gas exchange from a boreal legume grassland under organic and mineral nitrogen management

Tulasi Lakshmi Thentu [a,*], Daniel Forster [b], Yuan Li [a], Perttu Virkajärvi [a], Matthew Tom Harrison [c], Bhaskar Mitra [d], Jia Deng [e], Panu Korhonen [a], Narasinha Shurpali [a]

[a] Natural Resources Institute Finland (LUKE), Halolantie 35 A, 71750, Maaninka, Finland
[b] Toho University, Narashino Campus 2-2-1 Miyama, Funabashi, Chiba, 274-8510, Japan
[c] Tasmanian Institute of Agriculture, University of Tasmania, Launceston, TAS, 7248, Australia
[d] Information and Computational Sciences Department, The James Hutton Institute, Aberdeen, UK
[e] Earth Systems Research Center, Institute for the Study of Earth, Oceans and Space, University of New Hampshire, 39 College Road, Durham, NH, 03824, USA

ARTICLE INFO

Handling Editor: Jason Michael Evans

Keywords:
Carbon flux
Boreal grassland
HE-DNDC model
N_2O emissions
Net GHG balance

ABSTRACT

While grasslands are the cornerstone of Finnish livestock industries, practices for mitigating greenhouse gas (GHG) emissions are not well elucidated. Here, we used eddy covariance flux data measured on clover grassland in eastern Finland to calibrate and validate the Heat Exchange DNDC (HE-DNDC) model in response to synthetic mineral (Nmin) and organic manure (Norg) fertilizer. The study covered an entire grass/crop rotational cycle, and the study years were represented as R1 (May 20, 2017–May 19, 2018), R2 (May 20, 2018–May 19, 2019), and R3 (May 20, 2019–May 19, 2020). Simulated carbon flux was good/fair, evidenced by relatively high Mean Absolute Error (MAE) (11.1–20.9 kg C ha^{-1}) for both the treatments. For over 60 % of the observations, simulated biomass yield values were within one standard deviation of the measured values, indicating reasonable simulation accuracy. Cumulative measured N_2O emissions were 7.5 kg N ha^{-1} (Nmin) and 10.9 kg N ha^{-1} (Norg), with simulations closely matching Nmin (6.9 kg N ha^{-1}), but underestimating Norg (7.3 kg N ha^{-1}). Simulated net GHG balance (NGB) indicated that grasslands were a carbon sink for Norg in R1. During R2 and R3 (crop re-establishment) grasslands became a carbon source regardless of fertilizer treatment. We conclude that DNDC provides a reasonable estimation of the magnitude and timing of GHG fluxes associated with organic and mineral fertilizer application in boreal grasslands, although significant improvements are needed in simulating processes governing N_2O emissions.

1. Introduction

As a signatory of the Paris Agreement (UNFCCC, 2015), the Finnish Government aspires to carbon neutrality by 2035 (Ministry of Finance, 2024). The Finnish agrifood sector is the second largest source of greenhouse gas (GHG) emissions, contributing 13 % of national emissions in 2021 (Statistics Finland, 2024). Milk and beef production comprise the cornerstone of Finnish agriculture, with more than 4200 farms producing 2.17 B L of milk and 85 M kg of beef in 2023 (OSF, 2023).

Due to climatic and geological constraints, about 60 % of arable land in North Savo is allocated to grasslands, making it a key region for Finland's milk production. The grassland in this region are typically managed as 3–4 year rotational leys, with mixed perennial grasses (timothy + meadow fescue and or red clover) cultivated with barley (*Hordeum vulgare*) as a cover crop in the establishment year (OSF, 2023; Virkajärvi et al., 2015).

It is well known that nutrient and manure management have a significant influence on the GHG balance of the grassland systems (Rawnsley et al., 2018). Mineral fertilizers have been widely used to enhance biomass production, and there is a growing interest in organic fertilizer, such as digestate slurry from biogas production (Weiland, 2010). This shift has been partly driven by environmental concerns that the stored manure from livestock also contributes to GHG emissions (Pedersen and Hafner, 2023), and partly by potential for creation of circular nutrient cycles to reduce carbon footprints (Harrison and Liu, 2024; Li et al., 2023). As such, the development of technologies, skills, and practices to mitigate GHG emissions and improve carbon

* Corresponding author.
E-mail address: tulasi.thentu@luke.fi (T.L. Thentu).

https://doi.org/10.1016/j.jenvman.2025.126344
Received 24 December 2024; Received in revised form 15 June 2025; Accepted 21 June 2025
Available online 25 June 2025

sequestration will be essential for improving food production while minimising environmental impacts of agriculture (Liu et al., 2020). However, the heterogeneity of grassland production systems and the perennial nature of the grasses make field experiments challenging and costly (Bilotto et al., 2021).

To develop mitigation and adaptation strategies, there is thus growing demand for model-based paradigms to contrast the influence of various management scenarios on GHG emissions (Harrison, 2021). Process-based models, such as DNDC (i.e., DeNitrification-DeComposition) (Li et al., 1992), DayCent (Parton et al., 1998), STICS (Brisson et al., 2003), APSIM (Muleke et al., 2022), estimate GHG emissions via dynamic simulations of crop growth and biogeochemical processes, driven by climate factors, and human activities (Ogle et al., 2010). However, most models were developed for temperate or tropical climatic conditions, and thus have not been extensively evaluated for use in boreal regions, leading to uncertainties in their performance (Forster et al., 2022a).

Recent progress in the simulation of GHG flux from cold regions has been made using modified versions of DNDC. For example, Dutta et al. (2016) improved evapotranspiration predictions in a Canadian version of DNDC, while He et al. (2019, 2020) enhanced crop growth simulations by updating alfalfa (*Medicago sativa*) growth curves and incorporating winterkill effects. However, these versions provided limited mechanistic processes simulating snowpack and soil freeze–thaw dynamics. Cui and Wang (2019) further improved DNDC's performance by refining rain–snow partitioning, soil temperature estimation, and freeze–thaw simulation. Despite these enhancements, their model did not explicitly simulate key snowpack properties such as snow density changes and snow depth dynamics, which are critical for accurately modelling energy and heat transfers of snowpack and soil.

Most of the modelling studies have focused on Canadian boreal systems, and limited efforts have been made to test DNDC's performance under European boreal conditions. Particularly in Finland, where grasslands are intensively managed and experience strong seasonal snow cover, there remains a need to assess the model's robustness under different fertilizer treatments. Heat Exchange DNDC (HE-DNDC) model used in the current study, originally developed to enhance simulations of surface energy exchange, soil freeze-thaw cycles, and carbon gas fluxes in cold environments (Deng et al., 2014, 2020). This model incorporates a mechanistic soil thermal sub-model adapted from a permafrost modeling framework (Deng et al., 2014), explicitly simulating soil freeze–thaw cycles and snow cover as part of the soil–atmosphere energy exchange. Forster et al. (2022b) showed that when calibrated for Finnish boreal grasslands, modified DNDC (HE-DNDC) satisfactorily reproduced seasonal soil microclimate and GHG flux dynamics.

This study addresses this gap by calibrating and validating DNDC using high-precision eddy covariance (EC)-based GHG flux measurements from Finnish boreal grasslands, improving model accuracy for cold-region agricultural systems. This study evaluates the HE-DNDC model, performance with two specific objectives: (1) to assess simulated GHG emissions and biomass yields under organic and mineral fertilizer treatments, and (2) to compare annual GHG exchanges and net GHG balance (NGB) between the two treatments.

2. Materials and methods

2.1. Experimental site

The field study was established at Maaninka, located in eastern Finland (63°09′ 49″ N, 27°14′ 3″ E, 89 m a.s.l., Fig. 1). The region has an mean annual temperature (MAT) of 3.8 °C and mean annual precipitation (MAP) of 619 mm (1991–2020) (Finnish Meteorological Institute, 2024). During the experimental period from 2017 to 2019, the average temperature recorded was 5.1 °C with extremes of 25.0 °C and −26.5 °C. Annual precipitation was 613 mm in 2017, 515 mm in 2018, and 532 mm in 2019. The soil is silty loam (25 % ± 6 % clay, 53 % ± 9 % silt, 22 % ± 8 % sand) and classified as Haplic Cambisol (USDA) (Supplementary Table S1).

2.2. Management

The study site, covering 6.3 ha (280 m × 220 m), featured grass/crop

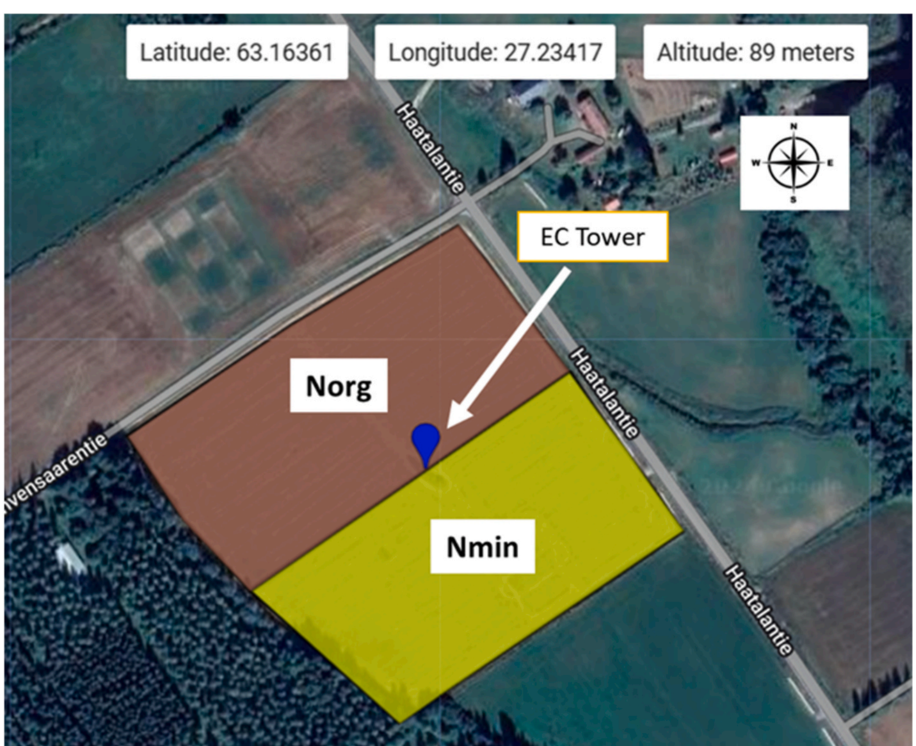

Fig. 1. Experimental setup of Nmin (Mineral Fertilizer) and Norg (Organic Manure) Treatments in Maaninka, Finland.

rotational cycles described as R1 (May 20, 2017–May 19, 2018), R2 (May 20, 2018–May 19, 2019), and R3 (May 20, 2019–May 19, 2020). A legume grassland was established in 2015 with a seed mix of timothy (*Phleum pratense* L., cv. Nuutti; 15 kg ha^{-1}), red clover (*Trifolium pratense* L., cv. Ilte; 5 kg ha^{-1}), and barley (cv. Kaarle; 160 kg ha^{-1}) as a cover crop, and sown using a tractor-mounted seed drill. Red clover reseeding (cv. Ilte; 3 kg ha^{-1}) was done in May 2017 (R1). Vegetation was cleared with glyphosate in autumn 2018, left bare over winter. Re-establishment in 2019 include timothy (15 kg ha^{-1}), red clover (3 kg ha^{-1}) and barley (160 kg ha^{-1}). Management details are provided in Table S2.

The site was divided into two sections: one receiving organic inputs (Norg) via biogas digestate slurry and the other receiving mineral inputs (Nmin) with chemical NPK fertilizer (Fig. 1). During R1 and R2, Nmin treatment received 106:28:50 kg NPK ha^{-1} annually. P, K, and half of the N were applied at the beginning of the growing season in spring, and remaining half of the N after the first cut. The Norg treatment received 98 (53 Soluble N): 13:83 kg NPK ha^{-1} annually after the first cut, applied using tractor-mounted spreaders. In R3, the Nmin treatment received 45:20:38 kg NPK ha^{-1}, while no manure was applied in the Norg treatment. Harvesting occurred biannually in R1 and R2 (late June and mid-August) and once in R3 (early August). Biomass was cut to 8 cm using a disc mower, followed by swathing, and baling.

2.3. Eddy covariance GHG flux measurements

The eddy covariance (EC) technique quantifies GHG flux by analysing the covariance between the gas concentrations and vertical wind velocities (Baldocchi, 2003). To measure CO_2, H_2O, and N_2O fluxes, the EC tower was equipped with an ultrasonic anemometer (R3-50; Gill Instruments Ltd., UK), an infrared gas analyzer (IRGA; LI-7000; LI-COR Biosciences), and a pulsed quantum cascade laser spectrometer (ARP-QC-TILDAS-76-CS; Aerodyne Research Inc., USA) (Shurpali et al., 2016). The EC tower was centrally located between the Nmin and Norg treatment plots (Fig. 1), so measured soil microclimate and carbon flux data represent a mixture of both treatments. N_2O fluxes were attributed to individual treatments based on prevailing wind direction (Li et al., 2023). EC fluxes were calculated from 30-min co-variances between the relevant scalar variables and vertical wind velocity, with due consideration given to the impact of humidity on temperature flux. Raw data were processed using EddyUH software (http://www.atm.helsinki.fi/Eddy_Covariance/EddyUHsoftware.php) and underwent quality control, spectral corrections, and gap-filling. Flux partitioning was performed using REddyProc (Reichstein et al., 2005). Missing meteorological data were filled using Maaninka weather station data (6 km from the site). Detailed instrumentation, calibration, and data processing methods are provided in Supplementary Section S1.

2.4. DNDC

2.4.1. Overview of the DNDC model

The DeNitrification-DeComposition (DNDC) model consists of six sub-models. (The soil climate, plant growth, and decomposition sub-models) are influenced by ecological drivers, and simulate soil environmental factors (e.g., soil temperature, moisture, pH, Eh) and content of substrates (e.g., NH_4^+, NO_3^- and dissolved organic carbon (DOC) (Li, 2000). These factors and substrates content drive the remaining three sub-models, denitrification, nitrification, and fermentation. These sub-models simulate the production, consumption and emissions of CO_2, CH_4 and N gases (i.e., NH_3, NO, N_2O, and N_2) from the plant-soil systems (Li, 2000).

2.4.2. Snow and soil freeze/thaw dynamics

Heat Exchange DNDC incorporates enhanced processes related to the reflection, absorption, and allocation of short and long wave radiation between canopy and ground surface. The model also includes advanced calculations of sensible and latent heat fluxes, allowing it to dynamically adjust based on snow cover (Deng et al., 2020). In addition, the model has been enhanced by incorporating a permafrost model to simulate snowpack dynamics, ground thermal dynamics, and soil freeze/thaw dynamics (Deng et al., 2014; Zhang et al., 2012). The effects of climate, vegetation, snowpack, ground features, and hydrological conditions on the soil thermal regime have been incorporated into the HE-DNDC on the basis of energy and water exchanges within soil-vegetation-atmosphere system (Deng et al., 2014). The model has been evaluated against field data of soil freeze/thaw dynamics and GHG fluxes in European boreal regions (Deng et al., 2014, 2015). The enhancements and evaluation make the HE-DNDC particularly suited for cold-region studies such as in Finland (Forster et al., 2022b) and the northeastern United States (Deng et al., 2020) where snow and freeze-thaw cycles significantly influence energy and carbon dynamics as well as GHG fluxes.

HE-DNDC simulates snowpack thickness using snow water equivalent and density profiles and calculates snowmelt based on surface energy excess and heat conduction from the ground (Zhang et al., 2003). Snow and soil temperatures are estimated as apparent temperatures and adjusted for phase changes by conserving energy during thawing and freezing. The fractions of ice and liquid water in each soil layer are dynamically updated, influencing both thermal properties and water movement (Zhang et al., 2003; Deng et al., 2014). Detailed description of the snow dynamics and freeze-thaw soil thermal processes in HE-DNDC is provided in the supplementary section S2.

2.4.3. Model evaluation and application

The model was run using daily climate data, including minimum and maximum temperatures (°C), rainfall (mm), humidity (%), wind speed (ms^{-1}), and solar radiation (MJ m^{-2}). Model calibration was carried out for crop-specific parameters including maximum biomass production (kg C ha^{-1} yr^{-1}), biomass fraction, biomass C:N ratio, thermal degree days to maturity, water demand (g water g^{-1} dry matter), nitrogen fixation index (crop N/N from soil), and optimum temperature (°C), as per Forster et al. (2022b). These crop parameters are summarized in Table S3 (a). No changes were made to model parameters related to energy and snow dynamics (Table S3 (b)). As shown in Fig. 3d, the simulated snowpack depth aligned well with observations, suggesting the original snow-related coefficients performed adequately under Finnish boreal conditions. The dataset from 20-May-2017 to 31-Dec-2018 was used for model calibration, while the dataset from 1-Jan-2019 to 31-May-2020 was used for model validation. The information pertaining to manure fertilization was updated as per the treatment (Table S4). The 'slurry animal waste' type was chosen as the closest available option to simulate Norg treatment in the HE-DNDC model. To stabilize the soil carbon stocks, the spin-up for the Nmin treatment was carried out by repeating the 2017 climate file 17 times, followed by the 2017–2020 experimental setup. For the organic treatment, 2016 climate file was repeated 17 times, followed by the 2017–2020 experimental setup. The results were studied for trends in C and N gas fluxes.

The model's performance against measured carbon and nitrogen gas fluxes was evaluated using four statistical measures: Mean Absolute Error (MAE), Root Mean Square Error (RMSE), Spearman's Rank Correlation Coefficient (ρ), and Percent Bias (pBias %). These measures provide insights into different aspects of model performance (Supplementary Section S3). Furthermore, model evaluation was conducted based on predetermined criteria (Table S5), which provides thresholds for each statistical measure, allowing for the classification of the model's performance as Excellent, Good, Fair, or Poor.

2.5. Net GHG balance (NGB)

NGB was calculated as the sum of NEE, harvested biomass carbon ($C_{harvest}$) and N_2O flux in C-equivalents ($GWP_{100} = 273$ for N_2O; Li et al., 2024), expressed in T CO_2 ha^{-1}. NGB was calculated separately for measured (NGB1 (Nmin); NGB2 (Norg)) and simulated (NGB3 (Nmin); NGB4 (Norg)) treatments. For Norg treatment, carbon added as organic fertilizer (Cnorg) was also included. Methane emissions were very low hence, they are disregarded in this analysis due to their expected minimal impact. The negative NBP values indicate C sequestration, while positive values represent C emission or release into the atmosphere.

For the Nmin treatment (Equations (1) and (2)):

$$NGB1\ (Nmin) = NEE + C_{harvest} + N_2O_{CO_2-eq} \tag{1}$$

$$NGB3\ (Nmin) = NEE\ (sim) + C_{harvest} + N_2O_{CO_2-eq} \tag{2}$$

For the Norg treatment (Equations (3) and (4)):

$$NGB1\ (Norg) = NEE + C_{harvest} - C_{Norg} + N_2O_{CO_2-eq} \tag{3}$$

$$NGB1\ (Norg) = NEE\ (sim) + C_{harvest} - C_{Norg} + N_2O_{CO_2-eq} \tag{4}$$

2.6. Statistical analysis

In the R script developed for this study (R version 4.2.0; R Core Team, 2022), several packages were utilized for data analysis, model performance evaluation, and visualization. To assess the model performance HydroGOF package was employed, while for data reshaping, cleaning, and manipulation (Wickham et al., 2023) the tidyverse collection (including tidyr) ware utilized. For data visualization, ggplot2 and ggpubr were primarily utilized, along with the egg package for layout adjustments.

3. Results

3.1. Climatic conditions during the study period

During the study period, MAT trended upward compared to the normal (1991–2020) (Fig. 2a). Among the experimental years, 2017 recorded the lowest mean daily temperatures (3.8 °C), followed by 2019, both of which were close to the normal. In contrast, 2018 and 2020 were the warmest years. The temperature variation was also reflected in the length of the growing season: 2017 had the shortest growing season of 136 days, while 2019 extended to 142 days and 2018 had the longest growing period of 155 days.

Compared with the normal (1991–2020), MAP during 2018 and 2019 was lower by about 17.0 and 14.1 %, respectively, classifying them as dry years, while 2017 and 2020 exceeded normal by 0.7 % and 9.5 %, respectively (Fig. 2b). This pattern was also observed during the growing seasons: 2017 recorded 284 mm, while 2018 and 2019 had 252 mm and 173 mm, respectively. Throughout the study period, high precipitation levels were observed from September to December (outside the growing season), with the lowest levels recorded during winter and early spring (January–April).

3.2. Model performance evaluation in simulating soil microclimate

The HE-DNDC Model closely predicted the soil temperatures throughout the experiment period. Although slight deviations were observed during winters with subfreezing temperatures, the model successfully simulated soil temperatures for both treatments (Fig. 3a).

Water-Filled Pore Space (WFPS) closely followed the trend of rainfall throughout the experimentation years, though there was wide fluctuation in measured data at 5 and 20 cm depth for both the treatments (Fig. 3b & c). During the winter months (January–April) when there is low precipitation and water was in freezing state, the measured WFPS was low. While in contrast, during the freezing and thawing events (May), there was a rise in measured WFPS at both depths (Fig. 3d).

Regarding the simulated results of WFPS at 5 cm and 20 cm depths, both overestimations and underestimations were observed throughout the growing period. At top layers the differences between treatments were more pronounced compared to the deeper layers. Additionally, the simulated WFPS values closely aligned with the measured data during the growing season, whereas larger discrepancies were evident during the winter months (Fig. 3b & c). The model captured snow dynamics well (RMSE ≈ 85 cm; d = 0.95, Table S6), slightly underestimating peak depths in R1 and R2, but overestimating in R3 (Fig. 3d).

3.3. Model performance evaluation in simulating CO_2 exchange

The comparative analysis of carbon fluxes for both the treatments showed a strong correlation across all variables (Table 1). For Nmin treatment: Gross Primary Productivity (GPP), Net Ecosystem Exchange (NEE), and Ecosystem Respiration (Reco) demonstrated a robust Spearman's rank correlation ($\rho > 0.7$, $p < 0.001$), indicating statistically significant strong monotonic relationships. However, MAE and RMSE values that fell into the higher range of the scale (MAE >20 for GPP; RMSE >20 for GPP and NEE), hence their performance was between fair to good. The pBias% values showed a slight tendency towards underestimation.

Similarly, the Norg treatment showed strong correlations, with lower bias for GPP (−19.5 %) but higher bias for NEE (−25.9 %) and Reco (−23.9 %) compared to Nmin treatment. Overall, the performance of the

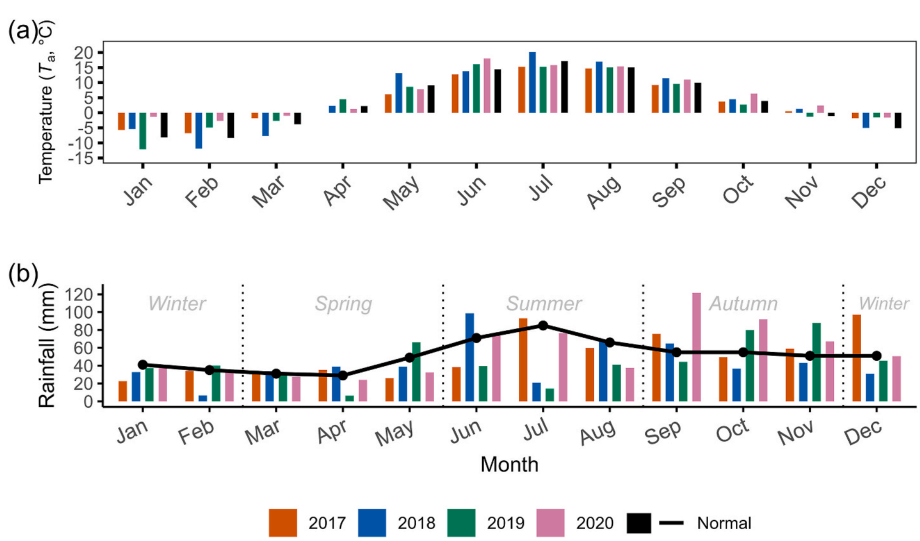

Fig. 2. Monthly mean air temperature (Ta, °C) and total monthly precipitation (mm) during 2017–2020 compared to the normal (1991–2020).

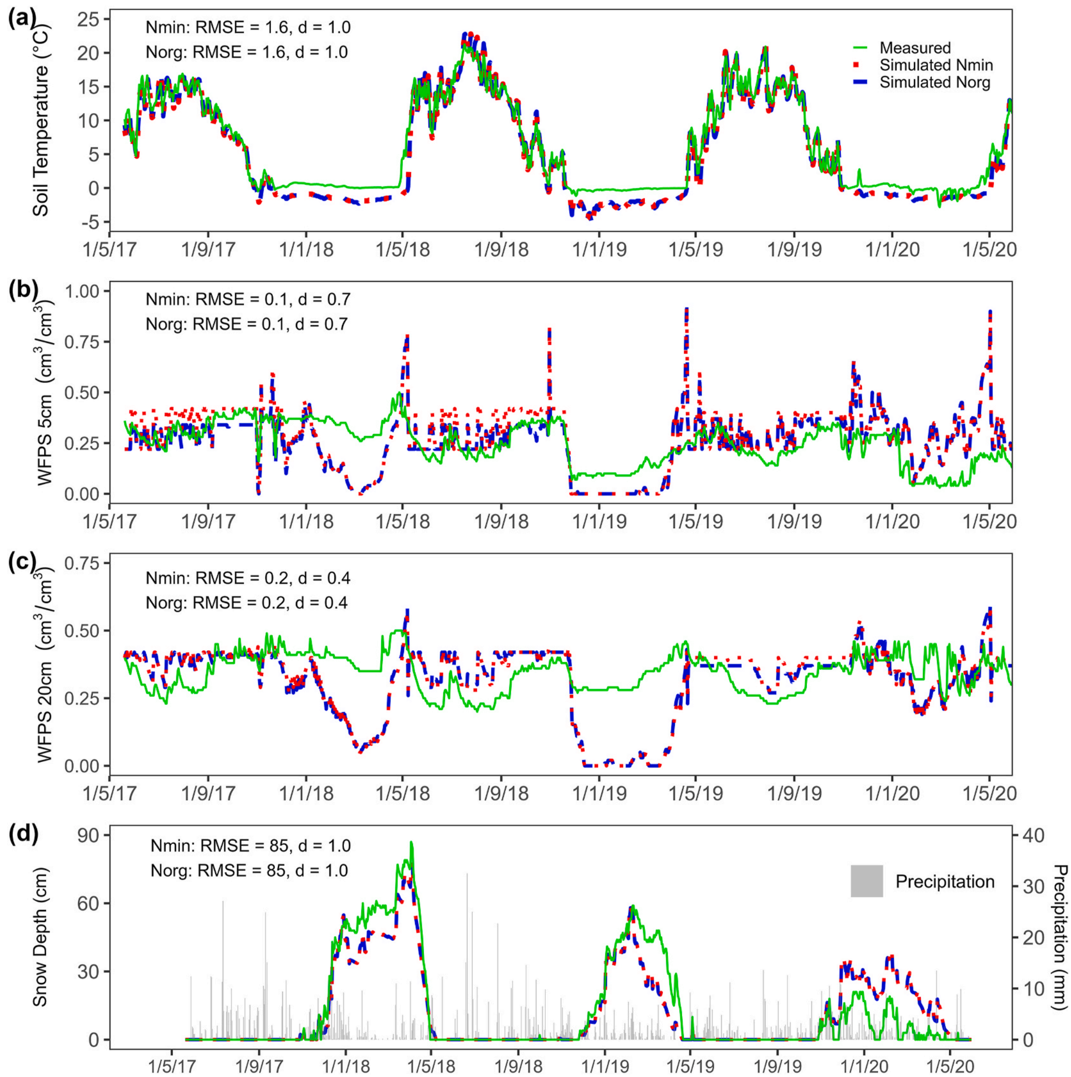

Fig. 3. Measured and simulated (Nmin and Norg) (a) soil temperature, (b) Water-Filled Pore Space (WFPS) at 5 cm depth, (c) WFPS at 20 cm depth, and (d) snow depth and precipitation from 2017 to 2020).

Table 1
Evaluation of simulated Nmin (mineral fertilizer) and Norg (organic manure) treatment outcomes against measured carbon exchange.

Treatment		Spearman's rank correlation (ρ)	MAE (kg C ha^{-1})	RMSE (kg C ha^{-1})	pBias %	Note
Nmin	GPP	0.8 ($p < 0.001$)	20.9	34.5	−21.0	Fair
	NEE	0.7 ($p < 0.001$)	16.3	26.3	−9.4	Good
	Reco	0.8 ($p < 0.001$)	11.2	14.4	−24.7	Fair
Norg	GPP	0.8 ($p < 0.001$)	20.9	34.5	−19.5	Fair
	NEE	0.7 ($p < 0.001$)	16.3	26.1	−25.9	Fair
	Reco	0.8 ($p < 0.001$)	11.1	14.5	−17.5	Good

Norg treatment also ranged from fair to good based on predefined evaluation criteria.

The model simulated similar trends for GPP and NEE for both Nmin and Norg treatments but showed delayed onset compared to measured data in R1 and R2 (Fig. 4a and b), especially in R2. In R3, more pronounced deviations were observed in NEE and Reco between treatments. Early in the R3 growing season, the model overestimated NEE and Reco for both treatments, while by the end of the season, simulations aligned more closely with measured. The magnitude of the differences was more pronounced for Reco compared to NEE.

Though the simulated carbon fluxes generally aligned with the measured data trends, discrepancies occurred during specific events, such as the thawing and freezing cycles at the onset of the growing season and the first cuts in R1 and R2. Contrary to measured trends, model failed to detect respiration until June 2018 (R2), whereas it overestimated respiration in May 2019 (R3). Throughout the experiment, Norg treatment consistently showed higher respiration than Nmin, especially during peak growing seasons. These differences were especially pronounced in R3, where simulated treatment values deviated significantly from measured data.

The comparison of annual carbon fluxes between the simulated and measured under the Nmin and Norg treatments reveals the ecosystem productivity and carbon exchange (Table 2). During R1 and R2, simulated GPP were significantly underestimated by 9.4 and 10.1 T CO_2 ha^{-1} for the Nmin and 8.7 and 9.5 T CO_2 ha^{-1} for Norg. These discrepancies were reduced in R3, with overestimations of 1.7 T CO_2 ha^{-1} and 1.8 T CO_2 ha^{-1} for Nmin and Norg treatment, respectively.

Simulated NEE for both the treatments exhibited underestimations in R2 and overestimations in R1 and R3. For the Nmin treatment, simulated NEE closely aligned with the measured data, with deviations ranging from 2.0 to 4.1 T CO_2 ha^{-1}. In contrast, deviations for the Norg treatment ranged from 1.6 to 7.8 T CO_2 ha^{-1}. Overall, the grassland served as a carbon sink, with negative NEE values recorded in both the measured

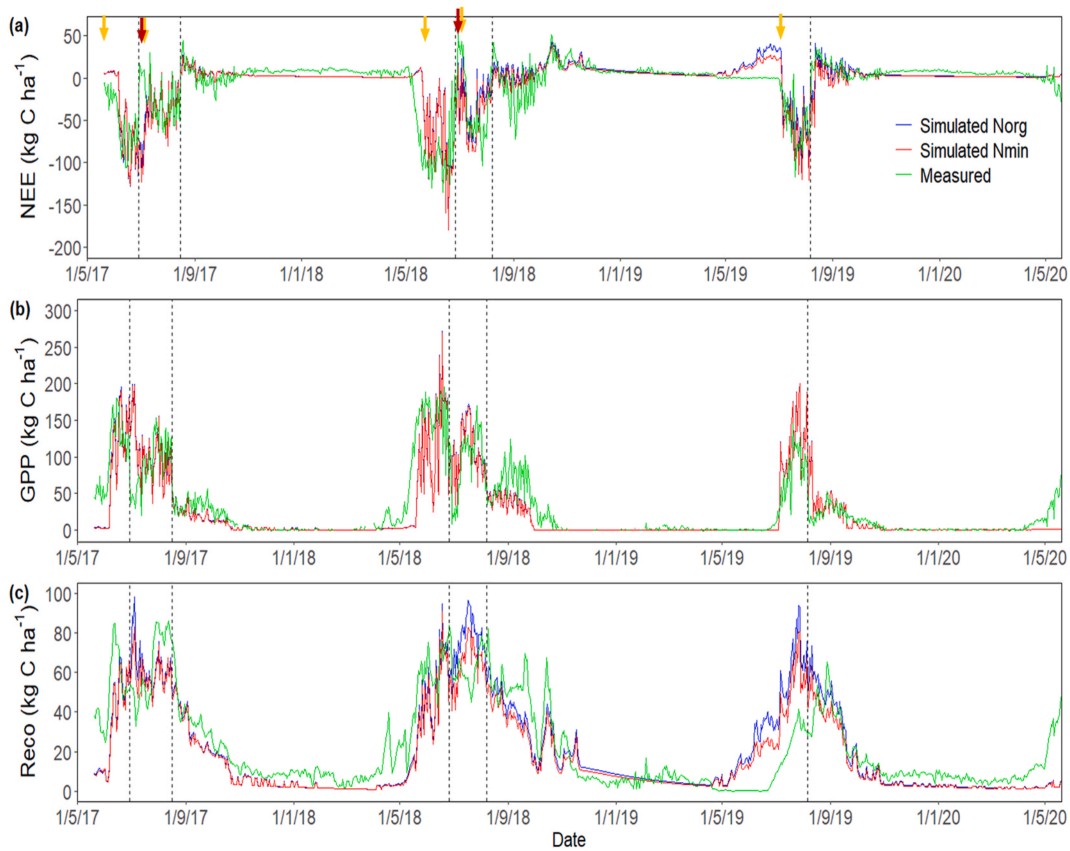

Fig. 4. Annual simulated and measured GPP, NEE, and Reco with harvesting events (dotted line), mineral fertilizer (yellow arrows), and organic manure applications (brown arrows).

Table 2
Comparison of total annual carbon exchanges under mineral and organic treatments across the rotational cycle.

Carbon exchanges (T CO_2 ha^{-1})	Study period	Measured data	Simulated Nmin treatment	Simulated Norg treatment	Difference between Measured and Nmin treatment	Difference between Measured and Norg treatment
GPP	R1	43.4	34.0	34.7	9.4	8.7
	R2	49.6	39.5	40.1	10.1	9.5
	R3	19.5	21.2	21.3	−1.7	−1.8
	Mean	**37.5**	**31.6**	**32.1**	**5.9**	**5.4**
NEE	R1	−8.1	−10.0	−9.6	2.0	1.6
	R2	−12.2	−8.2	−4.4	−4.1	−7.8
	R3	0.2	−2.0	2.3	2.1	−2.1
	Mean	**−6.7**	**−6.7**	**−3.9**	**0.0**	**−2.8**
Reco	R1	35.4	24.0	25.1	11.4	10.2
	R2	37.4	31.4	35.7	6.0	1.6
	R3	19.6	19.2	23.6	0.5	−3.9
	Mean	**30.8**	**24.9**	**28.1**	**5.9**	**2.7**

data (−6.7 T CO_2 ha^{-1}) and the simulated data (Nmin = −6.7 T CO_2 ha^{-1}, Norg = −3.9 T CO_2 ha^{-1}) throughout the study period.

Reco simulations for the Norg treatment aligned well with measured values, but the Nmin treatment showed significant underestimations. During R1, Reco was underestimated by 11.4 T CO_2 ha^{-1} (Nmin) and 10.2 T CO_2 ha^{-1} (Norg). But in R2, both treatments were underestimated, while in R3, Nmin closely matched measured values (deviation of 0.4 T CO_2 ha^{-1}), and the Norg treatment was overestimated by 3.9 T CO_2 ha^{-1}. Reco discrepancies were more pronounced than NEE, especially in R3.

3.4. Biomass yield

Throughout the experimental period, the HE-DNDC model generally overestimated biomass yield, except for the Norg treatment in R3, where it underestimated (Fig. 5). For Nmin treatment, the simulated mean biomass (2017–2019) was 4521 kg ha^{-1} ($t = -2.4$, $p = 0.04$; SD = 952 kg ha^{-1}) compared to measured mean of 3117 kg ha^{-1} (SD of 915 kg ha^{-1}). Similarly, for the Norg treatment, the simulated mean biomass was 4550 kg ha^{-1} ($t = -2.3$, $p = 0.05$; SD = 945 kg ha^{-1}), while the measured mean was 3026 kg ha^{-1} (SD = 1160 kg ha^{-1}).

For the two cut (harvest) system adopted here, the simulations for the first cut were close to measured biomass yields, while a notable disparity existed in the second cut. In R1, deviations in the second cut were 64 % (Nmin) and 122 % (Norg). In R2, simulated values were 158 % (Nmin) and 164 % (Norg) higher than measured values.

3.5. N_2O fluxes

The HE-DNDC model simulated N_2O flux with varying level of

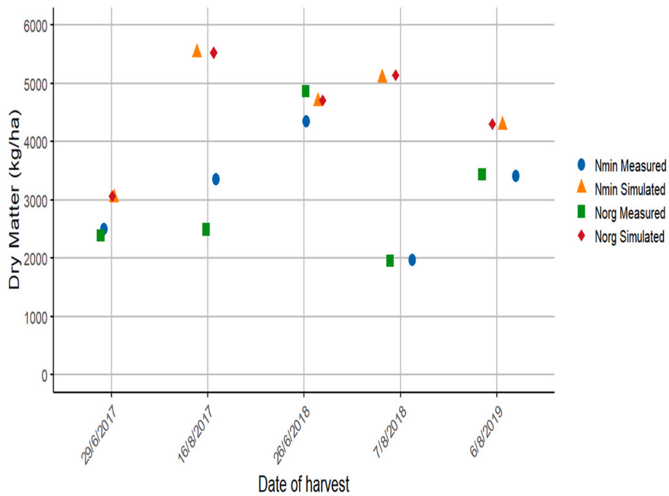

Fig. 5. Comparison of measured and simulated biomass production (DM kg ha^{-1}) for Nmin and Norg Treatments.

accuracy across treatments (Table S7). For the Nmin treatment during R1, the model's simulations (2.1 kg N ha^{-1}) for N_2O flux were within 11.6 % of the measured N_2O flux (1.9 kg N ha^{-1}). However, HE-DNDC model overestimated N_2O flux for the Norg treatment, with a simulated value of 3.5 kg N ha^{-1} against the measured 2.6 kg N ha^{-1}. In the following R2, the simulations for the Nmin treatment showed similar trend of overestimation, with 3.66 kg N ha^{-1} compared to the measured 2.2 kg N ha^{-1}. In the final rotational year of reestablishment (R3), model simulated very low N_2O emission (1.1 kg N ha^{-1}) for Nmin treatment. However, the model continued to underestimate the N_2O flux for Norg treatment during R2 and R3 with 2.1 kg N ha^{-1} and 1.7 kg N ha^{-1} respectively.

3.6. Net GHG balance (NGB)

The effect of measured and simulated nutrient treatments on NGB was assessed for the grassland rotation cycle (Fig. 6). In the Norg treatment, manure application initially made the ecosystem a minor carbon source (NGB2 (Norg) = 0.9 T CO_2 ha^{-1}, R1), transitioning to a carbon sink (NGB2 (Norg) = −2.2 T CO_2 ha^{-1}, R2). Simulations showed a reverse trend, with the system as a sink in R1 (NGB4 (Norg) = −0.3 T CO_2 ha^{-1}) and a source in R2 (NGB4 (Norg) = 5.3 T CO_2 ha^{-1}). In R3, measured (NGB2 (Norg) = 7.6 T CO_2 ha^{-1}) and simulated (NGB4 (Norg)

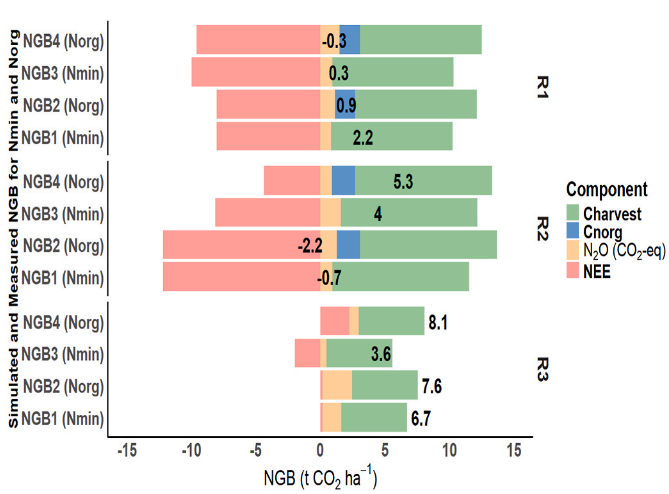

Fig. 6. Measured and simulated NGB for Nmin and Norg treatments across rotation cycles.

= 8.1 T CO_2 ha^{-1}) values closely aligned, showing the ecosystem as a strong carbon source.

A similar trend was observed with the Nmin treatment, where measured NGB values indicated ecosystem as a carbon sink (NGB1 (Nmin) = - 0.7 T CO_2 ha^{-1}) in R2, while in R1 and R3 it acted as a source. Simulated NBG indicated the ecosystem as a carbon source throughout the experimental period, with varying magnitudes. Notable gaps were observed in R2 and R3, where simulated NGB3 (Nmin) values were 4.0 T CO_2 ha^{-1} and 3.6 T CO_2 ha^{-1} respectively.

4. Discussion

Management and environmental conditions significantly influence GHG emissions and carbon dynamics in managed grasslands (Bilotto et al., 2021; Taylor et al., 2016). Here, we selected fertilizer as a management intervention because it is a simple lever that farmers can easily manipulate.

4.1. Climate impacts on grassland dynamics

Ambient temperatures during the study period significantly affected the length of the growing season, with higher temperatures correlating with extended growing seasons (Ergon et al., 2018). The early spring temperatures in R2 resulted in 19 days longer growing season than R1 and 13 days longer than R3. This temperature-driven extension of the growing season has significant implications for grassland management and productivity in the context of climate change (Ergon et al., 2018; Harrison, 2021).

Seasonal rainfall distribution, in addition to total annual precipitation, has proven crucial in influencing grass growth and biomass yield (Phelan et al., 2018), particularly in water-limited environments (Harrison et al., 2011). The contrasting effects of rainfall timing in 2017 (high rainfall outside the growing season) versus 2018–2019 (rainfall during the growing season) emphasize the importance of not just total precipitation but its timing in relation to plant growth stages. These results highlight the need for adaptive water management strategies in boreal grasslands, particularly during typically drier periods. Even though boreal ecosystems generally receive ample precipitation, our work suggests that climate-resilient management practices are very much necessary to maintain consistency of productivity, as this often has implications for farm business cash flow (Bilotto et al., 2023).

4.2. Model performance in simulating soil microclimate

The HE-DNDC model accurately simulated soil temperature dynamics, particularly at 5 cm depth, with minor deviations below 0 °C occurred during subfreezing periods., likely due to limitations in representing snow's insulating effects, despite advanced energy flux and freeze-thaw sub-models (Deng et al., 2020). However, Simulated WFPS, exhibited discrepancies, particularly at deeper layers i.e., 20 cm depth and during winter months, suggesting limitations in capturing soil moisture dynamics under freezing conditions and restricted water movement (Fig. 3c). Simulated snow depth closely matched observations across years, effectively capturing accumulation and melt patterns under both treatments (Fig. 3d). An exception was winter 2019–2020, when the model overestimated snow depth due to a typical snowfall. Still, model performance remained strong (RMSE ≈ 85 cm; d = 0.95).

Discrepancies in WFPS likely stem from the model's simplified linear root distribution, which fails to represent the complex rooting patterns of timothy (shallow-rooted), clover (deep-rooted), and barley (intermediate-rooted) across rotations (R1–R3). Underestimations during the non-growing season may also result from challenges in simulating impacts of soil freeze-thaw dynamics on soil water. For example, the model slightly underestimated soil temperature during most periods of the non-growing seasons (Fig. 3a). While the discrepancies in the soil temperature were small, the under-predictions could result in large differences between simulations and observations in soil water, given that soil water is very sensitive to the changes in soil temperature when it close to the soil water freezing point (Forster et al., 2022b). These findings align with previous studies highlighting DNDC's difficulties in modelling heterogeneous soils, rooting depths, and water redistribution (Pedersen et al., 2010; Uzoma et al., 2015; He et al., 2019, 2020).

4.3. Carbon flux and biomass yield simulations

Overall, the simulated carbon fluxes were reasonable, but significant discrepancies occurred during key management events, like grass cutting and fertilization (Fig. 4). R1 and R2 has very different weather patterns. R1 was typical, but R2 experienced an unusually early spring, about 20 days earlier than normal, making it an atypical year. The HE-DNDC model has limited phenological flexibility and fixed growth onset parameters likely prevented it from capturing this early seasonal shift, resulting in delayed simulations of fluxes. In contrast, R3, the simulated carbon fluxes occurred earlier than measured, likely due to its assumption of normal grass growth, whereas delays occurred due to seedling mortality and gap-filling. These temporal mismatches highlight the need to incorporate real-world disturbances for improved accuracy (Taylor et al., 2016). While Spearman's rank correlation indicated strong trend simulation, high MAE, RMSE, and pBias% values (Table 1) point to the need for enhanced precision. The model's monoculture assumption fails to capture complex interactions in mixed-species systems. Future improvements should focus on simulating post-harvest regrowth and plant component partitioning (Harrison et al., 2011) to enhance carbon flux predictions.

The model accurately simulated first-cut biomass yields but overestimated second-cut yields (Fig. 5), likely due to its monoculture perennial grass assumption, while the actual field comprised a mix of grasses (timothy, meadow fescue), legumes (red clover), and barley. The biogeochemical models often struggle to capture regrowth dynamics and species interactions in mixed-species systems (Van Oijen et al., 2020; Donaghy and Fulkerson, 1998). The slow recovery of timothy, which was dominant in the yield, likely contributed to the overestimation due to reproductive tillers losing their growing points after defoliation (Mäkiniemi et al., 2015). Refining the model to simulate mixed-species swards and varying regrowth capacities, together with interaction with grazing is essential. Comparing process-based models with different algorithms for canopy structure and botanical composition may help refine biomass yield simulations (Wallach et al., 2023).

4.4. N_2O flux and management effects

Our findings reveal significant impacts of fertilizer management on N_2O fluxes in boreal grasslands. For both the treatments, measured N_2O emissions were stable during R1 and R2 but were significantly higher in R3 than R2 by 55 % in the Nmin and 81 % in the Norg treatment (Table S7). This increase aligns with other studies indicating that soil disturbance (e.g., ploughing) and nutrient inputs promote microbial activity and organic matter mineralization, which drive nitrification and denitrification processes (Merbold et al., 2014; Li et al., 2022). As waterlogging causes spikes in N_2O, judicious management of snowmelt may be expected to dampen the seasonal quantum of GHG emissions (Liu et al., 2020).

The HE-DNDC model performed well in simulating total N_2O emissions for the Nmin treatment, with simulated values of 6.9 kg N ha^{-1} which closely match measured values i.e., 7.5 kg N ha^{-1}, resulting in an 8.3 % underestimation. For the Norg treatment, total N_2O emissions were underestimated by 33 % compared to the measured values of 10.9 kg N ha^{-1}. However, the model also underestimated emissions in R3, simulating 1.1 and 1.7 kg N ha^{-1} compared to measured values of 3.4 and 5.4 kg N ha^{-1} for the Nmin and Norg treatments, respectively. These discrepancies indicate that the model struggles to capture enhanced microbial activity and organic matter decomposition during re-establishment. The absence of fertilizer application in the Norg treatment during R3 further may have limited the model accuracy in simulation, as the model poorly accounted for residual organic inputs and their effect on denitrification (Christensen, 1983; Jones et al., 2007). Similar challenges have been reported, with DNDC underestimating N_2O emissions under 100 % manure treatments (Lv et al., 2020). These findings emphasize the need for model improvements to better capture the interactions between organic carbon, microbial activity, and N_2O production.

4.5. Net GHG balance

Net GHG Balance (NGB) analysis provides critical insights into carbon dynamics in boreal grasslands under different management regimes. Fertilizer management significantly influenced the ecosystem carbon balance, with measured data during R2 showing the grassland acted as a carbon sink (Fig. 6). The Norg treatment exhibited higher sink capacity, likely due to increased soil organic carbon inputs from organic manure (Zhu et al., 2021; Li et al., 2023). However, the grassland became a carbon source in R3 due to reestablishment activities, such as ploughing, which disturbed soil organic matter and enhanced mineralization, increasing CO_2 emissions (Hellebrand, 1998; Powlson et al., 2011). Lower biomass yields in R3 further reduced carbon uptake through photosynthesis, affecting NGB.

The model tended to simulate the Nmin treatment as a carbon source and the Norg treatment as a sink during R1. However, in R2, the model exhibited significant discrepancies, with simulated NGB values indicating the ecosystem as a strong source, while measured NGB values showed it acted as a sink for both the treatments. This divergence was primarily due to severe underestimations of NEE during this period, which ultimately impacted the ecosystem carbon balance. Additionally, underestimations of N_2O emissions also contributed to the discrepancies, though to a lesser extent compared to NEE.

In R3, while the model accurately represented both treatments as carbon sources, it underestimated NGB for the Nmin treatment and overestimated it for the Norg treatment. The underestimations in the Nmin treatment were due to underestimated NEE and N_2O emissions. In contrast, for the Norg treatment, despite underestimated N_2O emissions, the overestimated NEE, driven by an overestimation of Reco, led to the overestimation of NGB (Fig. 4).

These results suggest that future improvements in the model should focus on better representing the carbon dynamics associated with grassland establishment and reestablishment. Additionally, long-term studies that incorporate management practices impacting carbon inputs and outputs are necessary to refine model simulations and support sustainable management strategies in boreal grasslands.

5. Conclusion

The HE-DNDC model performed well in simulating GHG fluxes and carbon dynamics in boreal grasslands but showed limitations in capturing soil moisture at subfreezing temperatures, mixed-species dynamics, and nitrogen cycling during reestablishment. These findings highlight the need for further model refinements and field validation to improve simulations of GHG emissions, nutrient management, and biomass yields. Future research integrating diverse cropping systems and long-term management practices will enhance the model's utility for sustainable grassland management. Overall, the HE-DNDC model demonstrates strong potential to assess management strategies, supporting carbon neutrality and sustainability goals in dairy and beef farming.

CRediT authorship contribution statement

Tulasi Lakshmi Thentu: Writing – original draft, Visualization, Validation, Methodology, Investigation. **Daniel Forster:** Writing –

review & editing, Validation, Methodology. **Yuan Li:** Writing – review & editing, Methodology, Investigation. **Perttu Virkajärvi:** Writing – review & editing, Funding acquisition. **Matthew Tom Harrison:** Writing – review & editing. **Bhaskar Mitra:** Writing – review & editing. **Jia Deng:** Writing – review & editing, Validation. **Panu Korhonen:** Writing – review & editing. **Narasinha Shurpali:** Writing – review & editing, Supervision, Methodology, Investigation, Funding acquisition, Data curation, Conceptualization.

Declaration of competing interest

The authors declare that they have no known competing financial interests or personal relationships that could have appeared to influence the work reported in this paper.

Acknowledgements

This work was supported by the Ministry of Agriculture and Forestry of Finland (NC-Grass and ORMINURMI 2 projects), and the Regional Council of Pohjois-Savo (N-Fiksu project).

Appendix A. Supplementary data

Supplementary data to this article can be found online at https://doi.org/10.1016/j.jenvman.2025.126344.

Data availability

No data was used for the research described in the article.

References

Baldocchi, D.D., 2003. Assessing the eddy covariance technique for evaluating carbon dioxide exchange rates of ecosystems: past, present and future. Glob. Change Biol. 9, 479–492. https://doi.org/10.1046/j.1365-2486.2003.00629.x.

Bilotto, F., Harrison, M.T., Migliorati, M.D.A., Christie, K.M., Rowlings, D.W., Grace, P. R., Smith, A.P., Rawnsley, R.P., Thorburn, P.J., Eckard, R.J., 2021. Can seasonal soil N mineralisation trends be leveraged to enhance pasture growth? Sci. Total Environ. 772, 145031. https://doi.org/10.1016/j.scitotenv.2021.145031, 14.

Bilotto, F., Christie-Whitehead, K.M., Malcolm, B., Harrison, M.T., 2023. Carbon, cash, cattle and the climate crisis. Sustain. Sci. 18, 1795–1811. https://doi.org/10.1007/s11625-023-01323-2.

Brisson, N., Gary, C., Justes, E., Roche, R., Mary, B., Ripoche, D., Zimmer, D., Sierra, J., Bertuzzi, P., Burger, P., Bussière, F., Cabidoche, Y.M., Cellier, P., Debaeke, P., Gaudillère, J.P., Hénault, C., Maraux, F., Seguin, B., Sinoquet, H., 2003. An overview of the crop model STICS. Eur. J. Agron. 18, 309–332. https://doi.org/10.1016/S1161-0301(02)00110-7.

Christensen, S., 1983. Nitrous oxide emission from a soil under permanent grass: seasonal and diurnal fluctuations as influenced by manuring and fertilization. Soil Biol. Biochem. 15, 531–536.

Cui, G., Wang, J., 2019. Improving the DNDC biogeochemistry model to simulate soil temperature and emissions of nitrous oxide and carbon dioxide in cold regions. Sci. Total Environ. 687, 61–70. https://doi.org/10.1016/j.scitotenv.2019.06.054.

Deng, J., Li, C., Frolking, S., Zhang, Y., Bäckstrand, K., Crill, P., 2014. Assessing effects of permafrost thaw on C fluxes based on multiyear modeling across a permafrost thaw gradient at Stordalen, Sweden. Biogeosciences 11 (17), 4753–4770. https://doi.org/10.5194/bg-11-4753-2014.

Deng, J., Li, C., Frolking, S., 2015. Modeling impacts of changes in temperature and water table on C gas fluxes in an Alaskan peatland. J. Geophys. Res.: Biogeosciences 120 (7), 1279–1295. https://doi.org/10.1002/2014JG002880.

Deng, J., Xiao, J., Ouimette, A., Zhang, Y., Sanders-DeMott, R., Frolking, S., Li, C., 2020. Improving a biogeochemical model to simulate surface energy, greenhouse gas fluxes, and radiative forcing for different land use types in Northeastern United States. Glob. Biogeochem. Cycles 34, e2019GB006520. https://doi.org/10.1029/2019GB006520.

Donaghy, D.J., Fulkerson, W.J., 1998. Priority for allocation of water-soluble carbohydrate reserves during regrowth of *Lolium perenne*. Grass Forage Sci. 53 (3), 211–218. https://doi.org/10.1046/j.1365-2494.1998.00129.x.

Dutta, B., Smith, W.N., Grant, B.B., Pattey, E., Desjardins, R.L., Li, C., 2016. Model development in DNDC for the prediction of evapotranspiration and water use in temperate field cropping systems. Environ. Model. Software 80, 9–25. https://doi.org/10.1016/j.envsoft.2016.02.014.

Ergon, Å., Seddaiu, G., Korhonen, P., Virkajärvi, P., Bellocchi, G., Jørgensen, M., Østrem, L., Reheul, D., Volaire, F., 2018. How can forage production in Nordic and Mediterranean Europe adapt to the challenges and opportunities arising from climate change? Eur. J. Agron. 92, 97–106. https://doi.org/10.1016/j.eja.2017.09.016.

Finnish Meteorological Institute (FMI), 2024. Kuukausitilastot. https://www.ilmatieteenlaitos.fi/kuukausitilastot. (Accessed 11 October 2024) (In Finnish).

Forster, D., Deng, J., Harrison, M.T., Shurpali, N.J., 2022b. Simulating soil-plant-climate interactions and greenhouse gas exchange in boreal grasslands using the DNDC model. Land 11, 1947. https://doi.org/10.3390/land11111947.

Forster, D., Helama, S., Harrison, M.T., Rotz, C.A., Chang, J., Ciais, P., Pattey, E., Virkajärvi, P., Shurpali, N.J., 2022a. Use, calibration and verification of agroecological models for boreal environments: a review. Grassland Research 1, 14–30. https://doi.org/10.1002/glr2.12010.

Harrison, M.T., Evans, J.R., Dove, H., Moore, A.D., 2011. Recovery dynamics of rainfed winter wheat after livestock grazing 2. Light interception, radiation-use efficiency and dry-matter partitioning. Crop Pasture Sci. 62, 960–971. https://doi.org/10.1071/CP11235.

Harrison, M.T., 2021. Climate change benefits negated by extreme heat. Nat. Food 2, 855–856. https://doi.org/10.1038/s43016-021-00387-6.

Harrison, M.T., Liu, K., 2024. Holistic systems analyses accelerate progress towards sustainable development goals. Nat. Food 5, 544–545. https://doi.org/10.1038/s43016-024-00989-w.

He, W., Grant, B.B., Smith, W.N., VanderZaag, A.C., Piquette, S., Qian, B., Jing, Q., et al., 2019. Assessing alfalfa production under historical and future climate in Eastern Canada: DNDC model development and application. Environ. Model. Software 122, 104540. https://doi.org/10.1016/j.envsoft.2019.104540.

He, W., Dutta, B., Grant, B.B., Chantigny, M.H., Hunt, D., Bittman, S., Tenuta, M., et al., 2020. Assessing the effects of manure application rate and timing on nitrous oxide emissions from managed grasslands under contrasting climate in Canada. Sci. Total Environ. 716, 135374. https://doi.org/10.1016/j.scitotenv.2019.135374.

Hellebrand, H.J., 1998. Emission of nitrous oxide and other trace gases during composting of grass and green waste. J. Agric. Eng. Res. 69, 365–375. https://doi.org/10.1006/jaer.1997.0257.

Jones, S.K., Rees, R.M., Skiba, U.M., Ball, B.C., 2007. Influence of organic and mineral N fertilizer on N_2O fluxes from a temperate grassland. Agric. Ecosyst. Environ. 121, 74–83. https://doi.org/10.1016/j.agee.2006.12.006.

Li, C., Frolking, S., Frolking, T.A., 1992. A model of nitrous oxide evolution from soil driven by rainfall events: 1. Model structure and sensitivity. J. Geophys. Res. Atmos. 97 (D9), 9759–9776. https://doi.org/10.1029/92JD00509.

Li, C., 2000. Modeling trace gas emissions from agricultural ecosystems. Nutrient Cycl. Agroecosyst. 58, 259–276. https://doi.org/10.1023/A:1009859006242.

Li, Y., Moinet, G.Y.K., Clough, T.J., Whitehead, D., 2022. Organic matter contributions to nitrous oxide emissions following nitrate addition are not proportional to substrate-induced soil carbon priming. Sci. Total Environ. 851, 158274. https://doi.org/10.1016/j.scitotenv.2022.158274.

Li, Y., Korhonen, P., Kykkänen, S., Maljanen, M., Virkajärvi, P., Shurpali, N.J., 2023. Management practices during the renewal year affect the carbon balance of a boreal legume grassland. Front. Sustain. Food Syst. 7, 1158250. https://doi.org/10.3389/fsufs.2023.1158250.

Li, Y., Tian, H., Yao, Y., et al., 2024. Increased nitrous oxide emissions from global lakes and reservoirs since the pre-industrial era. Nat. Commun. 15, 942. https://doi.org/10.1038/s41467-024-45061-0.

Liu, K., Harrison, M.T., Ibrahim, A., Manik, S.M.N., Johnson, P., Tian, X., Meinke, H., Zhou, M., 2020. Genetic factors increasing barley grain yields under soil waterlogging. Food Energy Secur. 9, e238. https://doi.org/10.1002/fes3.238.

Lv, F., Song, J., Giltrap, D., Feng, Y., Yang, X., Zhang, S., 2020. Crop yield and N_2O emission affected by long-term organic manure substitution fertilizer under winter wheat-summer maize cropping system. Sci. Total Environ. 732, 139321. https://doi.org/10.1016/j.scitotenv.2020.139321.

Mäkiniemi, K., Hyrkäs, M., Virkajärvi, P., 2015. The origin and its effect on growing habits of the regrowth tillers of timothy and tall fescue in Finland. In: Nordic View to Sustainable Rural Development: Proceedings of the 25th Congress, Finland, 16–18 June 2015, pp. 121–126. In: https://llufb.llu.lv/conference/NJF/NJF_2015_Proceedings_Latvia-121-126.pdf.

Merbold, L., Eugster, W., Stieger, J., Zahniser, M., Nelson, D., Buchmann, N., 2014. Greenhouse gas budget (CO_2, CH_4, and N_2O) of intensively managed grassland following restoration. Glob. Change Biol. 20 (6), 1913–1928. https://doi.org/10.1111/gcb.12518.

Ministry of Finance, 2024. Finland's National reform programme 2024. European Commission. Available online: https://commission.europa.eu/document/download/f5f5116a-3e03-4439-9713-d0df77706790_en?filename=Finland-NRP-2024_EN.pdf.

Muleke, A., Harrison, M.T., de Voil, P., Hunt, I., Liu, K., Yanotti, M., Eisner, R., 2022. Earlier crop flowering caused by global warming alleviated by irrigation. Environ. Res. Lett. 17, 044032. https://doi.org/10.1088/1748-9326/ac5a66.

Ogle, S.M., Breidt, F.J., Easter, M., Williams, S., Killian, K., Paustian, K., 2010. Scale and uncertainty in modeled soil organic carbon stock changes for US croplands using a process-based model. Glob. Change Biol. 16, 810–820. https://doi.org/10.1111/j.1365-2486.2009.01951.x.

OSF, 2023. Official Statistics Finland. Natural Resources Institute Finland (Luke). https://statdb.luke.fi/PXWeb/pxweb/en/LUKE/LUKE_02%20Maatalous_04%20Tuotanto_02%20Maito-%20ja%20maitotuotetilasto/.

Parton, W., Hartman, M., Ojima, D., Schimel, D.S., 1998. DayCent and its land surface submodel: description and testing. Global Planet. Change 19, 35–48. https://doi.org/10.1016/S0921-8181(98)00040-X.

Pedersen, A., Zhang, K., Thorup-Kristensen, K., Jensen, L.S., 2010. Modelling diverse root density dynamics and deep nitrogen uptake–a simple approach. Plant Soil 32 (1–2), 493–510. https://doi.org/10.1007/s11104-009-0028-8.

Pedersen, J., Hafner, S.D., 2023. Ammonia emissions after field application of anaerobically digested animal slurry: literature review and perspectives. Agric. Ecosyst. Environ. 357, 108697. https://doi.org/10.1016/j.agee.2023.108697.
Phelan, D.C., Harrison, M.T., McLean, G., Cox, H., Pembleton, K.G., Dean, G.J., Parsons, D., do Amaral Richter, M.E., Pengilley, G., Hinton, S.J., Mohammed, C.L., 2018. Advancing a farmer decision support tool for agronomic decisions on rainfed and irrigated wheat cropping in Tasmania. Agric. Syst. 167, 113–124. https://doi.org/10.1016/j.agsy.2018.09.003.
Powlson, D.S., Whitmore, A.P., Goulding, K.W.T., 2011. Soil carbon sequestration to mitigate climate change: a critical re-examination to identify the true and the false. Eur. J. Soil Sci. 62 (1), 42–55. https://doi.org/10.1111/j.1365-2389.2010.01342.x.
R Core Team, 2022. R: a Language and Environment for Statistical Computing. R Foundation for Statistical Computing, Vienna, Austria. URL. https://www.R-project.org/.
Rawnsley, R., Dynes, R.A., Christie, K.M., Harrison, M.T., Doran-Browne, N.A., Vibart, R., Eckard, R., 2018. A review of whole farm-system analysis in evaluating greenhouse-gas mitigation strategies from livestock production systems. Anim. Prod. Sci. 58, 980–989. https://doi.org/10.1071/AN15632.
Reichstein, M., Falge, E., Baldocchi, D., Papale, D., Aubinet, M., Berbigier, P., et al., 2005. On the separation of net ecosystem exchange into assimilation and ecosystem respiration: review and improved algorithm. Glob. Change Biol. 11, 1424–1439. https://doi.org/10.1111/j.1365-2486.2005.001002.x.
Shurpali, N.J., Rannik, Ü., Jokinen, S., Lind, S., Biasi, C., Mammarella, I., Peltola, O., Pihlatie, M., Hyvönen, N., Räty, M., Haapanala, S., Zahniser, M., Virkajärvi, P., Vesala, T., Martikainen, P.J., 2016. Neglecting diurnal variations leads to uncertainties in terrestrial nitrous oxide emissions. Sci. Rep. 6, 25739. https://doi.org/10.1038/srep25739.
Statistics Finland, 2024. Greenhouse gas emissions in Finland: National inventory document 2024. https://stat.fi/media/uploads/tup/khkinv/fi_nid_eu_2022_2024-03-15_v2.pdf.
Taylor, C.A., Harrison, M.T., Telfer, M., Eckard, R., 2016. Modelled greenhouse gas emissions from beef cattle grazing irrigated leucaena in northern Australia. Anim. Prod. Sci. 56 (2–3), 594–604. https://doi.org/10.1071/AN15575.
UNFCCC (United Nations Framework Convention on Climate Change), 2015. Paris agreement. In: https://unfccc.int/process-and-meetings/the-paris-agreement/the-paris-agreement.
Uzoma, K.C., Smith, W., Grant, B., Desjardins, R.L., Guo, X., Hanis, K., Tenuta, M., Goglio, P., Li, C., 2015. Assessing the effects of agricultural management on nitrous oxide emissions using flux measurements and the DNDC model. Agric. Ecosyst. Environ. 206, 71–83. https://doi.org/10.1016/j.agee.2015.03.014.
Van Oijen, M., Barcza, Z., Confalonieri, R., Korhonen, P., Kröel-Dulay, G., Lellei-Kovács, E., Louarn, G., Louault, F., Martin, R., Moulin, T., Movedi, E., Picon-Cochard, C., Rolinski, S., Viovy, N., Wirth, S.B., Bellocchi, G., 2020. Incorporating biodiversity into biogeochemistry models to improve prediction of ecosystem services in temperate grasslands: review and roadmap. Agronomy 10 (2), 259. https://doi.org/10.3390/agronomy10020259.
Virkajärvi, P., Rinne, M., Mononen, J., Niskanen, O., Järvenranta, K., Sairanen, A., 2015. Dairy production systems in Finland. In: Grassland and Forages in High Output Dairy Farming Systems: Proceedings of the 18th Symposium of the European Grassland Federation, Wageningen, the Netherlands, 15-17 June 2015, 51. https://www.europeangrassland.org/fileadmin/documents/Infos/Printed_Matter/Proceedings/EGF2015.pdf.
Wallach, D., Palosuo, T., Thorburn, P., Mielenz, H., Buis, S., Hochman, Z., Gourdain, E., Andrianasolo, F., Dumont, B., Ferrise, R., Gaiser, T., Garcia, C., Gayler, S., Harrison, M., Hiremath, S., Horan, H., Hoogenboom, G., Jansson, P.-E., Jing, Q., Justes, E., Kersebaum, K.-C., Launay, M., Lewan, E., Liu, K., Mequanint, F., Moriondo, M., Nendel, C., Padovan, G., Qian, B., Schütze, N., Seserman, D.-M., Shelia, V., Souissi, A., Specka, X., Srivastava, A.K., Trombi, G., Weber, T.K.D., Weihermüller, L., Wöhling, T., Seidel, S.J., 2023. Proposal and extensive test of a calibration protocol for crop phenology models. Agron. Sustain. Dev. 43 (4), 46. https://doi.org/10.1007/s13593-023-00900-0, 1-14.
Weiland, P., 2010. Biogas production: current state and perspectives. Appl. Microbiol. Biotechnol. 85, 849–860. https://doi.org/10.1007/s00253-009-2246-7.
Wickham, H., Vaughan, D., Girlich, M., 2023. Tidyr: tidy, messy data, Version 1.3.0. https://tidyr.tidyverse.org.
Zhang, Y., Chen, W., Cihlar, J., 2003. A process-based model for quantifying the impact of climate change on permafrost thermal regimes. J. Geophys. Res. Atmos. 108 (D22). https://doi.org/10.1029/2002JD003354.
Zhang, Y., Sachs, T., Li, C., Boike, J., 2012. Upscaling methane fluxes from closed chambers to eddy covariance based on a permafrost biogeochemistry integrated model. Glob. Change Biol. 18 (5), 1428–1440. https://doi.org/10.1111/j.1365-2486.2011.02587.x.
Zhu, Y., Merbold, L., Leitner, S., Wolf, B., Pelster, D., Goopy, J., Butterbach-Bahl, K., 2021. Interactive effects of dung deposited onto urine patches on greenhouse gas fluxes from tropical pastures in Kenya. Sci. Total Environ. 761, 143184. https://doi.org/10.1016/j.scitotenv.2020.143184.